Striatal dopamine transporter and receptor availability correlate with relative cerebral blood flow measured with [11C]PE2I, [18F]FE-PE2I and [11C] raclopride PET in healthy individuals

My Jonasson[1,2] ⓘ, Andreas Frick[3], Patrik Fazio[4], Olof Hjorth[5], Torsten Danfors[1,6], Jan Axelsson[7] ⓘ, Lieuwe Appel[1,6], Tomas Furmark[5], Andrea Varrone[4] and Mark Lubberink[1,2]

Abstract

The aim of this retrospective study was to investigate relationships between relative cerebral blood flow and striatal dopamine transporter and dopamine D2/3 availability in healthy subjects. The data comprised dynamic PET scans with two dopamine transporter tracers [11C]PE2I (n = 20) and [18F]FE-PE2I (n = 20) and the D2/3 tracer [11C]raclopride (n = 18). Subjects with a [11C]PE2I scan also underwent a dynamic scan with the serotonin transporter tracer [11C] DASB. Binding potential (BP_{ND}) and relative tracer delivery (R_1) values were calculated on regional and voxel-level. Striatal R_1 and BP_{ND} values were correlated, using either an MRI-based volume of interest (VOI) or an isocontour VOI based on the parametric BP_{ND} image. An inter-tracer comparison between [11C]PE2I BP_{ND} and [11C]DASB R_1 was done on a VOI-level and simulations were performed to investigate whether the constraints of the modeling could cause correlation of the parameters. A positive association was found between BP_{ND} and R_1 for all three dopamine tracers. A similar correlation was found for the inter-tracer correlation between [11C]PE2I BP_{ND} and [11C]DASB R_1. Simulations showed that this relationship was not caused by cross-correlation between parameters in the kinetic model. In conclusion, these results suggest an association between resting-state striatal dopamine function and relative blood flow in healthy subjects.

Introduction

There is an increased interest in dual-biomarker approaches with positron emission tomography (PET) to aid in differential diagnosis of patients with neurodegenerative disorders, where both blood flow and, for example, receptor or transporter availability, amyloid load or other characteristics are determined from the same PET scan.[1–5] There are several PET tracers that target the dopamine system, and three of them are [11C]PE2I, [18F]FE-PE2I and [11C]raclopride. While [11C]PE2I and [18F]FE-PE2I bind to the dopamine transporter (DAT),[6–8] [11C]raclopride binds to dopamine D2/3 receptors[9] and all three tracers show

[1]Department of Surgical Sciences, Nuclear Medicine and PET, Uppsala University, Uppsala, Sweden
[2]Medical Physics, Uppsala University Hospital, Uppsala, Sweden
[3]Department of Medical Sciences, Psychiatry, Uppsala University, Uppsala, Sweden
[4]Department of Clinical Neuroscience, Centre for Psychiatry Research, Karolinska Institutet, Stockholm, Sweden
[5]Department of Psychology, Uppsala University, Uppsala, Sweden
[6]Medical Imaging Centre, Uppsala University Hospital, Uppsala, Sweden
[7]Department of Radiation Sciences, Radiation Physics, Umeå University, Umeå, Sweden

Corresponding author:
My Jonasson, Uppsala University Hospital, 75185 Uppsala, Sweden.
Email: my.jonasson@uu.se

a high affinity and selectivity for their respective target.[10,11] A dynamic PET scan with either of these tracers can give information both on the non-displacable binding potential (BP_{ND}), as a measure of DAT or dopamine D2/3 receptor availability, and relative tracer delivery (R_1).[12–14] For tracers that are not limited by blood flow, the extraction in target and reference tissue can be assumed to be similar and R_1 can serve as a proxy of relative cerebral blood flow (rCBF).[15]

It is important that the two measures are independent to ensure that they can be interpreted correctly when both are used in the differential diagnosis of neurodegenerative disorders, such as suggested for example for parkinsonism with [^{11}C]PE2I.[1] This can be further complicated when using simplified binding measures instead of BP_{ND}. For example, the semi-quantitative standardized uptake value ratio (SUVR) estimate, a simplified measure of target availability used as a surrogate for BP_{ND}, can be affected by delivery of the tracer which has been shown for several tracers including [^{11}C]PE2I and [^{18}F]FE-PE2I.[16] This can affect longitudinal measures of SUVR if changes in blood flow occur over time, which for example has been shown for amyloid imaging[17] where increased tracer binding with progressing disease is counteracted by decreases in regional CBF, resulting in underestimation of disease progression if SUVR was assumed to represent tracer binding only.

In addition, lack of fulfillment of the underlying assumptions of the simplified reference tissue model could possibly result in cross-correlations of model parameters.[13,18] In a previous study, Cumming et al. (2013) found a relationship between the dopamine D2/3 specific tracer [^{18}F]fallypride binding and a surrogate marker for CBF.[19] They suggested that this might be due to high extraction fraction of the tracer and that the observed relationship might be attributed to early specific binding. However, neither [^{11}C]PE2I, [^{18}F]FE-PE2I or [^{11}C]raclopride have as high extraction fraction as [^{18}F]fallypride and the BP_{ND} values based on tracer kinetic modeling from a longer scan duration are assumed not to be dependent on blood flow. In a more recent simultaneous PET/MR study in non-human primates, Sander et al. showed that controlled changes in the cerebral blood flow did not alter the [^{11}C]raclopride or [^{18}F]fallypride binding, and they concluded that the hemodynamic and receptor binding parameters are independent.[20]

The purpose of this retrospective study was to investigate the relation between resting-state striatal DAT or dopamine D2/3 availability and rCBF using dynamic [^{11}C]PE2I, [^{18}F]FE-PE2I and [^{11}C]raclopride PET data.

Materials and methods

Subjects

In this retrospective study, data of 58 healthy controls previously included in three different studies were used.[21–23] The data comprised dynamic PET scans with [^{11}C]PE2I and [^{11}C]DASB (n = 20, mean ± SD age 39.4 ± 13.1 years), [^{18}F]FE-PE2I (n = 20; mean ± SD age 61.8 ± 6.9 years) and [^{11}C]raclopride (n = 18; mean ± SD age 25.2 ± 4.8 years). Written informed consent was obtained from all subjects and each study was approved by the regional board of medical ethics and radiation safety committee in Uppsala or Stockholm according to the ethical standards of the Helsinki Declaration of 1975 (and as revised in 1983) and according to the Swedish Law on ethics review for research in humans.

Data acquisition

Dynamic [^{11}C]PE2I PET scans were acquired on an ECAT Exact HR+ scanner (Siemens/CTI) at Uppsala University Hospital (Sweden).[21] A 10 min transmission scan, with three retractable ^{68}Ge rotating line sources, was performed for attenuation correction prior to the emission scans. [^{11}C]PE2I was administered intravenously as a bolus of 350–400 MBq, simultaneously with the start of the emission scan and the data were acquired in 22 time frames over 80 min (4 × 60 s, 2 × 120 s, 4 × 180 s, 12 × 300 s). In addition, these subjects also underwent a dynamic [^{11}C]DASB PET scan, on the same day, using identical injection and scanning procedures. The [^{11}C]DASB data were acquired in 22 time frames over 60 min (1 × 60 s, 4 × 30 s, 3 × 60 s, 4 × 120 s, 2 × 180 s, 8 × 300 s). The dynamic [^{11}C]PE2I and [^{11}C]DASB scans were reconstructed using ordered subset expectation maximization (OSEM) with 6 iterations and 8 subsets and a 4 mm Hanning post-filter with a matrix size of 128 × 128 × 63 and a voxel size of 2.06 × 2.06 × 2.43 mm^3.

[^{18}F]FE-PE2I PET scans were acquired on a High Resolution Research Tomograph (HRRT) system (Siemens/CTI) at the PET-center at Karolinska Institutet (Stockholm, Sweden).[22] For attenuation correction, a 6-min transmission scan with a single ^{137}Cs source, was acquired before each emission scan. A 93 min dynamic PET acquisition was obtained after bolus injection of about 200 MBq [^{18}F]FE-PE2I. The images were reconstructed into 37 time frames (8 × 10 s, 5 × 20 s, 4 × 30 s, 4 × 60 s, 4 × 180 s, 12 × 360 s) using OSEM with 10 iterations and 16 subsets, including

modeling of the point spread function, with a matrix size of $256 \times 256 \times 207$ and an isotropic voxel size of 1.22 mm.

Dynamic [11C]raclopride PET scans were acquired during 90 min in an integrated Signa PET/MR scanner (GE Healthcare) at the Uppsala University PET/MR facility (Sweden).[23] A bolus infusion protocol was used with a total amount of radioactivity of approximately 400 MBq and a k_{bol} of 107 min.[24] The [11C]raclopride images were reconstructed into 5-min frames using OSEM with 4 iterations and 28 subsets, including resolution recovery and a 5 mm gauss post-filter, with a matrix size of $128 \times 128 \times 89$ and a voxel size of $2.34 \times 2.34 \times 2.78$ mm^3. An atlas-based method, provided by the manufacturer, was used for attenuation correction. The scan started with 50 min PET data collection in resting-state, which were followed by a challenge. This, however, is outside the scope of this investigation and only data from the first 45 min of the [11C]raclopride PET scan are used in this paper.

All appropriate corrections were applied when reconstructing the PET images. In addition, each subject received an anatomical T1-weighted magnetic resonance image (MRI) scan on either a 3T Achieva scanner (Philips Healthcare), a 3T Discovery MR750 scanner (GE Healthcare) or a 3T Signa PET-MR scanner (GE Healthcare).

Image analysis

Volumes of interest based quantification. The dynamic PET data were realigned to correct for inter-frame subject movement using VOIager (GE Healthcare, Uppsala, Sweden). A rigid transformation was used to co-register each subject's MRI scan to an early summed PET image and the MR-images were segmented into gray matter, white matter and CSF using SPM8 (Statistical Parametric Mapping; fil.ion.ucl.ac.uk/spm). An automated VOI template, implemented in the PVElab software,[25] was used to define grey matter VOIs on the co-registered MR-images. Three bilateral VOIs were included for each subject: cerebellum, putamen and caudate. The VOIs were applied to the dynamic PET data to extract time activity curves (TACs) from which BP_{ND} and R_1 were calculated using the simplified reference tissue model (SRTM)[13] with grey matter cerebellum as reference region. In addition, for [11C]raclopride data acquired using the bolus infusion protocol, BP_{ND} was also estimated as the ratio between the activity concentration in the target region and the reference region minus 1 at 35–45 min p.i. The relationship between BP_{ND} and R_1 from the same PET scan was assessed for [11C]PE2I, [18F]FE-PE2I and [11C]raclopride. The SRTM modeling was performed using in-house developed software in Matlab (The Mathworks, Natick, USA).

Voxel-wised quantification. Parametric images, showing BP_{ND} and R_1 at the voxel level, were computed using receptor parametric mapping (RPM),[26] a basis function implementation of SRTM. A set of one hundred basis functions were predefined for each scan, with a discrete set of values for the exponential variable ranging from 0.01–0.5 min^{-1} for both [11C]PE2I and [18F]FE-PE2I and 0.01–0.2 min^{-1} for [11C]raclopride. Weights were included to account for the different counts in each frame. Before the voxel-level analysis, the [18F]FE-PE2I images were smoothed with a 5 mm gauss filter and a highly constrained back projection (HYPR) method[27] were applied to ensure a similar spatial resolution as the [11C]PE2I and [11C]raclopride images and to reduce noise in the images. Also, a 5 mm gauss filter was applied to the [11C]raclopride data before the analysis for noise reduction. Parametric image calculations were done in Matlab.

To preclude influence of partial volume effects on the correlation between R_1 and BP_{ND} in the caudate and putamen, an isocontour VOI of the striatum was defined on the parametric BP_{ND} image for each scan. A threshold of 70% of the maximum BP_{ND} value was applied individually for every subject and tracer and only voxels with BP_{ND} exceeding the threshold were included in the isocontour analysis. The images were masked using the gray matter, white matter and CSF segmentation, to only include pixels within the brain. Mean BP_{ND} values within the isocontour volume were obtained and the same isocontour VOIs were transferred to the corresponding parametric R_1 image to derive a mean striatal R_1 value.

The parametric images were normalized to MNI standard space by first normalizing the co-registered MR-images in SPM12, and then applying the transformation matrices to each parametric image. The normalized images were resampled to 2 mm voxels and smoothed with an 8 mm gauss filter.

Inter-tracer relationship. In addition to the intra-tracer relationship, VOI-based correlations between [11C]PE2I BP_{ND} and [11C]DASB R_1, as well as [11C]PE2I R_1 and [11C]DASB R_1, were also assessed to investigate the inter-tracer relationship within the same subjects. This was evaluated for the 20 subjects receiving both [11C]PE2I and [11C]DASB.

Simulations

Simulations were performed to investigate a possible cross-correlation between the parameters due to the

modelling. One hundred reference and target TACs were simulated using the two-tissue compartment model with a constructed plasma input curve, random parameters and rate constants determined based on literature values.[28] A small amount of random noise was added to the TACs to match the magnitude of noise seen in actual cerebellum and striatal TACs. The parameters were chosen to reflect the behavior of high [11C]PE2I binding in striatum, with BP_{ND} ranging from 10 to 20 and R_1 between 1 and 1.5. For the refence TACs the rate constants were chosen as $K_{1ref} = 0.29–0.31$, $k_{2ref} = 0.09–0.11$, $k_{3ref} = 0.019–0.021$ and $k_{4ref} = 0.059–0.061$. For the target TACs, K_1 was calculated as $K_{1ref} \times R_1$ and k_2 as $k_{2ref} \times R_1$ with an added extra $\pm 10\%$ variation, k_4 was set to a constant of 0.03 and random k_3 was calculated as $k_3 \times BP_{ND}$. The chosen parameters challenge the assumptions for SRTM, having reference TACs that can not be described by a one tissue compartment model (1TCM), since this is the case for [11C]PE2I.[28–30] In addition, the simulations were also performed with an optimal SRTM reference region with k_{3ref} and k_{4ref} set to zero. The TACs were analyzed using SRTM and a set of 100 R_1 and BP_{ND} values were obtained for each simulation.

Statistical analysis

Pearson's correlation test was performed to assess the relationship between the [11C]PE2I, [18F]FE-PE2I and [11C]raclopride BP_{ND} and corresponding R_1 values using GraphPad Prism (GraphPad Software, San Diego, Ca, USA) and the square of the correlation coefficient (R^2) was calculated. These intra-tracer relationships were done for both the VOI-based and voxel-wise quantification of BP_{ND} and R_1. Correlation maps, showing R^2 at a voxel level, were calculated between the normalized parametric R_1 and BP_{ND} images for [11C]PE2I, [18F]FE-PE2I and [11C]raclopride, applying

thresholds at $BP_{ND} > 1$ and p-value < 0.05. To investigate effects of the size of the VOIs on the BP_{ND} values, multiple linear regression analysis was performed in Matlab with BP_{ND} as the dependent variable and R_1, size of the cerebellum VOI and size of the isocontour VOI as independent variable. Inter-tracer relationship were assessed by means of VOI-based correlation between [11C]PE2I BP_{ND} and [11C]DASB R_1, as well as [11C]PE2I R_1 and [11C]DASB R_1, in the same subjects. In the simulation study, Pearsons correlations between BP_{ND} and R_1 were assessed for the non-zero and zero k_{3ref} and k_{4ref} datasets.

Results

VOI analysis

Significant correlations were found between the template VOI-based SRTM R_1 and BP_{ND} in caudate and putamen, for [11C]PE2I, [18F]FE-PE2I and [11C] raclopride, Figure 1. [18F]FE-PE2I showed the highest correlation ($R^2 = 0.72$), followed by [11C]raclopride ($R^2 = 0.59$) and [11C]PE2I ($R^2 = 0.52$). BP_{ND} estimated during the equilibrium analysis for [11C]raclopride showed a similar correlation to SRTM R_1 ($R^2 = 0.64$) and a very high agreement between SRTM BP_{ND} and equilibrium BP_{ND} was found ($R^2 = 0.95$, slope $= 1.08$). The p-values for all correlations were <0.0001. Mean SRTM BP_{ND} and R_1 values for the caudate and putamen for all three tracers are given in Table 1.

Isocontour VOIs

In Figure 2, examples of parametric RPM BP_{ND} and R_1 images are shown for [11C]PE2I, [18F]FE-PE2I and [11C]raclopride. The striatum was delineated, in both sets of images, with the isocontour VOI based on the 70% of the maximum BP_{ND} value. The relationships
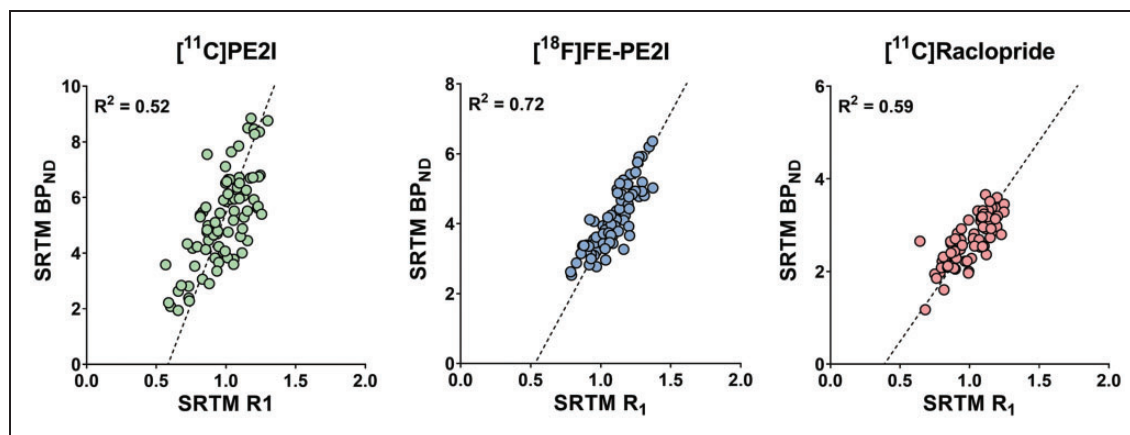

Figure 1. Relationship between VOI-based SRTM R_1 and BP_{ND} values in putamen and caudate for [11C]PE2I, [18F]FE-PE2I and [11C] raclopride.

Table 1. Mean BP_{ND} and R_1 values in caudate, putamen and the 70% isocontour VOI for all three tracers.

	Caudate		Putamen		Isocontour	
	BP_{ND}	R_1	BP_{ND}	R_1	BP_{ND}	R_1
$[^{11}C]PE2I$	4.70 ± 1.27	0.86 ± 0.11	6.32 ± 1.64	1.15 ± 0.08	9.30 ± 1.13	1.21 ± 0.10
$[^{18}F]FE-PE2I$	3.65 ± 0.67	0.99 ± 0.10	4.52 ± 0.82	1.18 ± 0.10	4.64 ± 0.83	1.16 ± 0.10
$[^{11}C]raclopride$	2.32 ± 0.38	0.88 ± 0.09	3.05 ± 0.33	1.13 ± 0.06	3.48 ± 0.33	1.17 ± 0.06
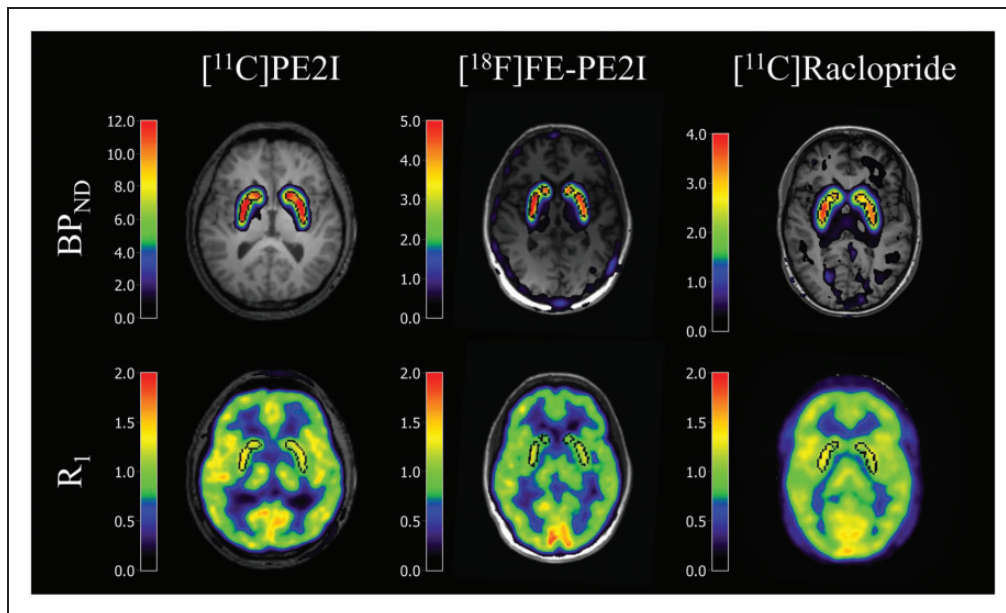
Figure 2. Parametric BP_{ND} and R_1 images of $[^{11}C]PE2I$, $[^{18}F]FE-PE2I$ and $[^{11}C]raclopride$. Images are overlaid on the subject's co-registered MRI scan and the edges of the 70% isocontour VOIs are delineated in black over the striatum.
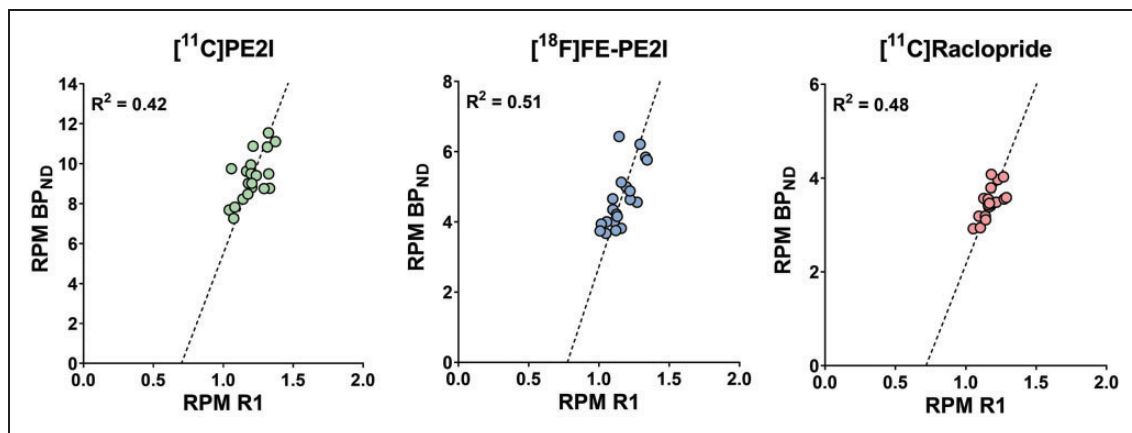
Figure 3. Relationship between RPM R_1 and BP_{ND} values extracted with a 70% isocontour VOI over the striatum in the parametric images of $[^{11}C]PE2I$, $[^{18}F]FE-PE2I$ and $[^{11}C]raclopride$.

between the R_1 and BP_{ND} values extracted from the parametric images using the isocontour VOIs are given in Figure 3. The correlation was highest for $[^{18}F]FE-PE2I$ ($R^2 = 0.51$) and slightly lower for $[^{11}C]PE2I$ ($R^2 = 0.42$) and $[^{11}C]raclopride$ ($R^2 = 0.48$). The correlations were lower than for the SRTM analysis of the anatomical VOIs of the putamen and caudate, but significant for all three tracers (p-value ≤ 0.002). Mean RPM BP_{ND} and R_1 values for all three tracers are given in Table 1.
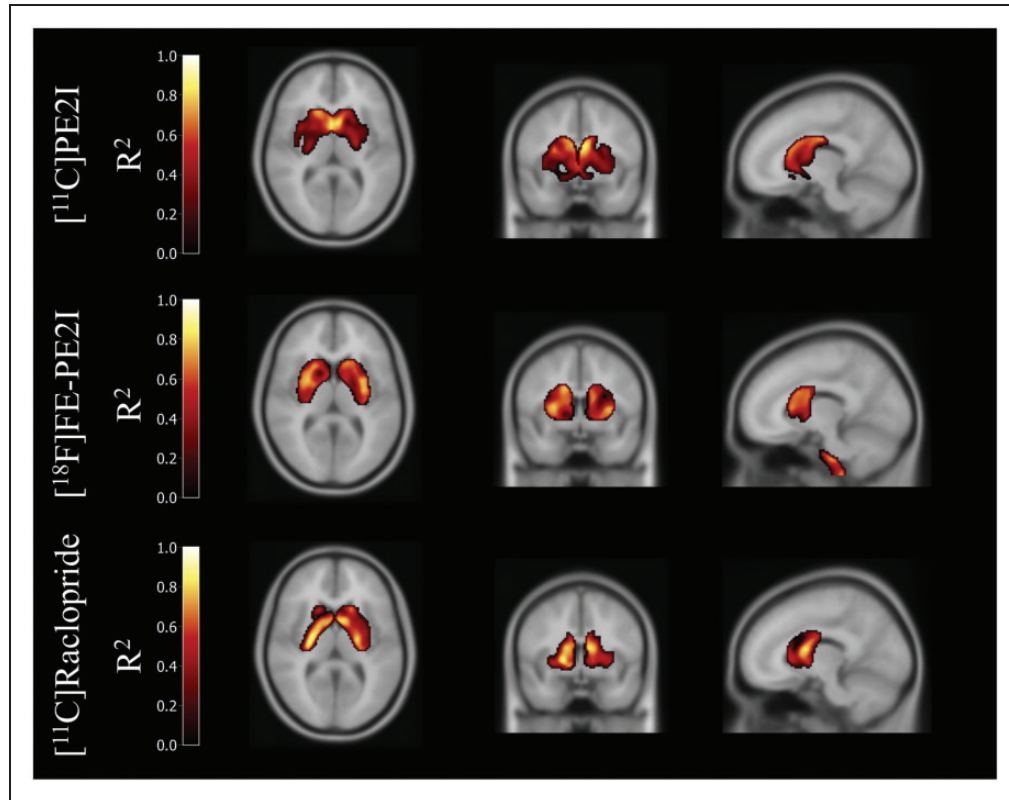
Figure 4. Voxel-wise correlation coefficient (R^2) between normalized R_1 and BP_{ND} parametric images for [^{11}C]PE2I, [^{18}F]FE-PE2I and [^{11}C]raclopride, applying thresholds at $BP_{ND} > 1$ and p-value < 0.05.

Multilinear and voxel-wise regression analysis

In Figure 4, the voxel-wise R^2 maps are displaying the correlation between R_1 and BP_{ND}, with a threshold p-value of 0.05, for [^{11}C]PE2I, [^{18}F]FE-PE2I and [^{11}C] raclopride. In the multilinear regression analysis, with R_1, isocontour VOI size and cerebellum VOI size as independent variables, R_1 came out as the strongest predictor of BP_{ND} for [^{11}C]PE2I and [^{18}F]FE-PE2I, $p < 0.001$. For [^{11}C]PE2I, the cerebellum VOI size also came out as a significant predictor with $p = 0.04$, but a linear regression between cerebellum VOI size and BP_{ND} did not show significant correlation, $p = 0.82$. For [^{11}C] raclopride, R_1 did not show a significant association with BP_{ND}, $p = 0.098$, but instead, the isocontour VOI size was the only significant predictor of BP_{ND} with a p-value < 0.001 and a negative correlation with BP_{ND}.

Inter-tracer correlation

The relationship between [^{11}C]DASB R_1 and [^{11}C]PE2I BP_{ND} is given in Figure 5. The correlation was similar to the intra-tracer relationship of R_1 and BP_{ND} of [^{11}C] PE2I ($R^2 = 0.54$, p-value < 0.0001). In addition, there was a high inter-tracer correlation between the R_1 values from [^{11}C]PE2I and [^{11}C]DASB, ($R^2 = 0.90$, slope $= 1.01$), also shown in Figure 5.

Simulations

The relationships between the computed R_1 and BP_{ND} values from the simulated TACs, for both sets of parameters, are given in Figure 6. For the non-zero k_{3ref} and k_{4ref}, the resulting R_1 and BP_{ND} values were approximately in the same range as found in striatal regions for healthy controls with [^{11}C]PE2I. These values were about 50% lower than for the simulations with a k_{3ref} and k_{4ref} set to zero, since SRTM underestimates BP_{ND} in case of a violation of the 1TC kinetics in the reference TAC.[31] However, the correlations between R_1 and BP_{ND} from the simulation analyses were much lower than the results from clinical data, regardless of reference TAC kinetics ($R^2 = 0.07$, p-value $= 0.006$ and $R^2 = 0.03$, p-value $= 0.09$).

Discussion

In this retrospective study, the relationship between relative blood flow and availability of DAT and dopamine receptors in the striatum was investigated for [^{11}C]PE2I, [^{18}F]FE-PE2I and [^{11}C]raclopride PET. The correlation between R_1 and BP_{ND} was assessed using SRTM analysis with MRI-based VOIs as well as isocontour VOIs based on maximum BP_{ND} values
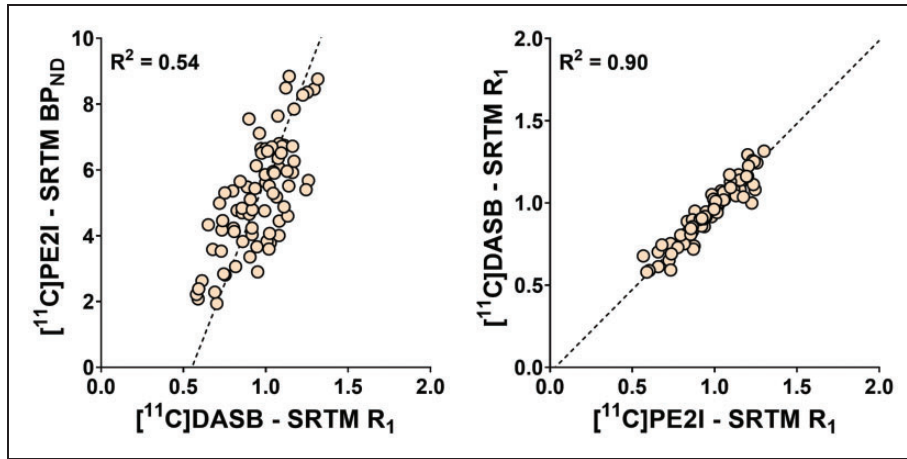
Figure 5. Inter-tracer correlation of VOI-based SRTM values in putamen and caudate between [11C]DASB R_1 and [11C]PE2I BP_{ND} and [11C]DASB R_1 and [11C]PE2I R_1.

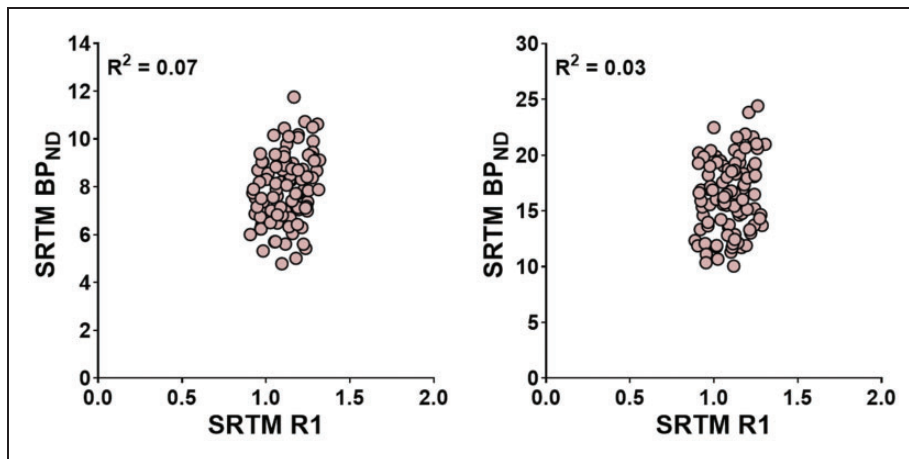**Figure 6.** Relationship between SRTM R_1 and BP_{ND} values based on simulations of high bindning [11C]PE2I time activity curves with non-zeros k_{3ref} and k_{4ref} (left) and zero k_{3ref} and k_{3ref} (right).

of parametric images computed with RPM. In addition, an inter-tracer correlation was evaluated between [11C]PE2I BP_{ND} and [11C]DASB R_1 within the same subjects and simulations was performed to further clarify any link between the parameters due to the modeling.

The VOI-based analysis showed a substantial, positive correlation between R_1 and BP_{ND} in caudate and putamen, for all three dopamine tracers. As such a correlation was not expected, this raised the question whether there is a true physiological relationship. One possible explanation is the occurrence of different degrees of partial volume effects. Another explanation might be that the automatically generated VOIs based on the subject's individual MRI, although having a good anatomical fit, are not covering the actual uptake of the tracer in striatum. As a consequence, the BP_{ND} and R_1 values in the same subjects will be underestimated. This will induce a larger variation between subjects, and altogether causing a correlated underestimation of the outcome parameters.

To preclude the effect of potential partial volume effects or a mismatch between the VOIs and the PET uptake, isocontour VOIs were defined on the parametric BP_{ND} images. The positive correlations between R_1 and BP_{ND}, extracted from the parametric images using isocontour VOIs, were slightly lower than when using the anatomical VOIs but the correlations were still substantial for all three dopamine tracers. The result of the multilinear regression showed that there was no significant contribution of striatal VOI sizes to the relation between R_1 and BP_{ND} for either [11C]PE2I or [18F]FE-PE2I. This outcome precludes that VOI-size dependent partial volume effects could explain the R_1 and BP_{ND} relationship in these cases. A further support for this finding was demonstrated by the voxel-level regression

analysis between normalized R_1 and BP_{ND} parametric images, with resulting R^2 maps, which showed a clear correlation in the striatum for all three tracers.

The correlation found may be enhanced by the higher BP_{ND} and R_1 values in putamen than caudate, as seen in Table 1. However, correlations remain significant for the isocontour VOI where the two regions are combined, as well as at the voxel level. It remains to be seen how strong the relationship is with tracers for which putamen does not have the highest target density.

In contrast to the multivariate analysis of [11C]PE2I and [18F]FE-PE2I, for [11C]raclopride, R_1 did not show a significant association to BP_{ND}, but instead the striatal isocontour VOI size was a significant predictor with a negative correlation to BP_{ND}. This negative relationship might be explained by the fact that the parametric [11C]raclopride images were noisy and had to be filtered to enable the use of isocontour VOIs. However, the SRTM results for [11C]raclopride (Figure 1) were based on unfiltered TAC data and show a substantial, positive correlation between R_1 and BP_{ND}. For [11C]raclopride, a bolus infusion protocol was used which makes it possible to determine BP_{ND} as the ratio between the target region and the reference region, and should be a measure independent of flow. The correlation between SRTM R_1 and equilibrium BP_{ND} was similar to that found between SRTM R_1 and SRTM BP_{ND}, which further supports the findings in this work.

The correlation that was found between [11C]PE2I BP_{ND} and [11C]DASB R_1 was in accordance with the intra-tracer relationship for [11C]PE2I BP_{ND} and R_1. As the correlation between [11C]PE2I BP_{ND} and an independent measurement of R_1 from the [11C]DASB scan was similar to the relationship found between BP_{ND} and R_1 from the same [11C]PE2I scan, it indicates that this correlation is not due to a model induced coupling of the parameters. The opposite relationship, between [11C]PE2I R_1 and serotonin transporter [11C]DASB binding, was also observed with an $R^2 = 0.78$ (data not shown). This would of course also imply a high agreement between the relative blood flow measures within subjects, which indeed also was the case, with very high correlation and agreement between [11C]PE2I R_1 and [11C]DASB R_1, with $R^2 = 0.9$ and a slope very close to one.

The relationship between R_1 and BP_{ND} found for the clinical data could not be reproduced in the simulation. Thus, this is an additional confirmation that these findings are not depending on the kinetic modelling. Although a significance level less than 0.05 was found, the correlation was still very low. [11C]PE2I does not fulfill all the underlying assumptions for SRTM, and the simulated parameters were chosen to reflect that. However, adjusting the parameters to not violate the assumptions of a 1TCM reference kinetics, with $k_{3\ ref}$ and $k_{4\ ref}$ set to zero, only lowered the correlation coefficient and increased the p-value.

The physiological implications of the findings in this work remain to be clarified. For example, a more active dopamine system might require a higher striatal perfusion or the activity of the dopamine system is limited by the blood flow in healthy individuals. The present study assessed the relationship between dopamine transporter and receptor availability and relative cerebral blood flow, but it provides no information on the relation with absolute cerebral blood flow. Hence, the relevance of this finding should be subject of further investigations to assess quantitative measures of blood flow, optimally with [15O]water PET, in connection with dopamine PET investigations. In addition, it would be interesting to explore the association between the blood flow and the dopamine system in specific patient groups with impaired dopamine function.

Conclusion

A positive association was found between relative blood flow and availability of DAT and dopamine D2/3 receptors in the striatum using kinetic analysis of dynamic PET scans with [11C]PE2I, [18F]FE-PE2I and [11C]raclopride. A relationship between DAT availability and relative blood flow from two different tracers, which was observed between [11C]PE2I BP_{ND} and [11C]DASB R_1, further enhances the relevance of this finding. Model-related cross-correlation between parameters could not explain this relationship. These results suggest an association between resting-state striatal dopamine function and relative blood flow in healthy subjects.

Declaration of conflicting interests

The author(s) declared no potential conflicts of interest with respect to the research, authorship, and/or publication of this article.

Authors' contributions

AV, ML and MJ designed and conceptualized the study; AF, OH, TF, AV and PF collected the data; MJ and ML analysed

the data and drafted the manuscript. MJ, AF, PF, OH, TD, JA, LA, TF, AV and ML contributed to the scientific process, interpretation of the results, critically revised the manuscript and approved the final version.

ORCID iDs

My Jonasson 🆔 https://orcid.org/0000-0003-3259-2613
Jan Axelsson 🆔 https://orcid.org/0000-0002-3731-3612

References

1. Appel L, Jonasson M, Danfors T, et al. Use of 11C-PE2I PET in differential diagnosis of Parkinsonian disorders. *J Nucl Med* 2015; 56: 234–242.
2. Meyer PT, Hellwig S, Amtage F, et al. Dual-biomarker imaging of regional cerebral amyloid load and neuronal activity in dementia with PET and 11C-labeled Pittsburgh compound B. *J Nucl Med* 2011; 52: 393–400.
3. Van Laere K, Clerinx K, D'Hondt E, et al. Combined striatal binding and cerebral influx analysis of dynamic 11C-raclopride PET improves early differentiation between multiple-system atrophy and Parkinson disease. *J Nucl Med* 2010; 51: 588–595.
4. Wolters EE, van de Beek M, Ossenkoppele R, et al. Tau PET and relative cerebral blood flow in dementia with Lewy bodies: a PET study. *Neuroimage Clin* 2020; 28: 102504.
5. Rodriguez-Vieitez E, Leuzy A, Chiotis K, et al. Comparability of [(18)F]THK5317 and [(11)C]PIB blood flow proxy images with [(18)F]FDG positron emission tomography in Alzheimer's disease. *J Cereb Blood Flow Metab* 2017; 37: 740–749.
6. Halldin C, Erixon-Lindroth N, Pauli S, et al. [(11)C]PE2I: A highly selective radioligand for PET examination of the dopamine transporter in monkey and human brain. *Eur J Nucl Med Mol Imaging* 2003; 30: 1220–1230.
7. Sasaki T, Ito H, Kimura Y, et al. Quantification of dopamine transporter in human brain using PET with 18F-FE-PE2I. *J Nucl Med* 2012; 53: 1065–1073.
8. Varrone A, Tóth M, Steiger C, et al. Kinetic analysis and quantification of the dopamine transporter in the nonhuman primate brain with 11C-PE2I and 18F-FE-PE2I. *J Nucl Med* 2011; 52: 132–139.
9. Farde L, Hall H, Ehrin E, et al. Quantitative analysis of D2 dopamine receptor binding in the living human brain by PET. *Science* 1986; 231: 258–261.
10. Emond P, Garreau L, Chalon S, et al. Synthesis and ligand binding of nortropane derivatives: N-substituted 2beta-carbomethoxy-3beta-(4′-iodophenyl)nortropane and N-(3-iodoprop-(2E)-enyl)-2beta-carbomethoxy-3beta-(3′,4′-disubstituted phenyl)nortropane. New high-affinity and selective compounds for the dopamine transporter. *J Med Chem* 1997; 40: 1366–1372.
11. Hall H, Köhler C, Gawell L, et al. Raclopride, a new selective ligand for the dopamine-D2 receptors. *Prog Neuropsychopharmacol Biol Psychiatry* 1988; 12: 559–568.
12. Jonasson M, Appel L, Engman J, et al. Validation of parametric methods for [^{11}C]PE2I positron emission tomography. *Neuroimage* 2013; 74: 172–178.
13. Lammertsma AA and Hume SP. Simplified reference tissue model for PET receptor studies. *Neuroimage* 1996; 4: 153–158.
14. Odano I, Varrone A, Hosoya T, et al. Simplified estimation of binding parameters based on image-derived reference tissue models for dopamine transporter bindings in non-human primates using. *[Am J Nucl Med Mol Imaging* 2017; 7: 246–254.
15. Chen YJ, Rosario BL, Mowrey W, et al. Relative 11C-PiB delivery as a proxy of relative CBF: quantitative evaluation using single-session 15O-Water and 11C-PiB PET. *J Nucl Med* 2015; 56: 1199–1205.
16. Jonasson M, Langaas GL, Appel L, et al. Blood flow dependence of early [11C]PE2I and [18F]FE-PE2I PET SUVR measurements used in the differential diagnosis of Parkinsonian disorders. *Eur J Nucl Med Mol Imaging* 2018; 45: 303–304.
17. van Berckel BN, Ossenkoppele R, Tolboom N, et al. Longitudinal amyloid imaging using 11C-PiB: methodologic considerations. *J Nucl Med* 2013; 54: 1570–1576.
18. Salinas CA, Searle GE and Gunn RN. The simplified reference tissue model: model assumption violations and their impact on binding potential. *J Cereb Blood Flow Metab* 2015; 35: 304–311.
19. Cumming P, Xiong G, la Fougère C, et al. Surrogate markers for cerebral blood flow correlate with [^{18}F]-fallypride binding potential at dopamine D(2/3) receptors in human striatum. *Synapse* 2013; 67: 199–203.
20. Sander CY, Mandeville JB, Wey HY, et al. Effects of flow changes on radiotracer binding: simultaneous measurement of neuroreceptor binding and cerebral blood flow modulation. *J Cereb Blood Flow Metab* 2019; 39: 131–146.
21. Hjorth OR, Frick A, Gingnell M, et al. Expression and co-expression of serotonin and dopamine transporters in social anxiety disorder: a multitracer positron emission tomography study. *Mol Psychiatry* 2021; 26: 3970–3979.
22. Brumberg J, Kerstens V, Cselényi Z, et al. Simplified quantification of [(18)F]FE-PE2I PET in parkinson's disease: discriminative power, test-retest reliability and longitudinal validity during early peak and late pseudo-equilibrium. *J Cereb Blood Flow Metab* 2021; 41: 1291–1300.
23. Frick A, Björkstrand J, Lubberink M, et al. Dopamine and fear memory formation in the human amygdala. *Mol Psychiatry* 2022; 27: 1704–1711.
24. Carson RE, Breier A, de Bartolomeis A, et al. Quantification of amphetamine-induced changes in [11C]raclopride binding with continuous infusion. *J Cereb Blood Flow Metab* 1997; 17: 437–447.
25. Svarer C, Madsen K, Hasselbalch SG, et al. MR-based automatic delineation of volumes of interest in human brain PET images using probability maps. *Neuroimage* 2005; 24: 969–979.
26. Gunn RN, Lammertsma AA, Hume SP, et al. Parametric imaging of ligand-receptor binding in PET using a simplified reference region model. *Neuroimage* 1997; 6: 279–287.
27. Christian BT, Vandehey NT, Floberg JM, et al. Dynamic PET denoising with HYPR processing. *J Nucl Med* 2010; 51: 1147–1154.

28. Jucaite A, Odano I, Olsson H, et al. Quantitative analyses of regional [11C]PE2I binding to the dopamine transporter in the human brain: a PET study. *Eur J Nucl Med Mol Imaging* 2006; 33: 657–668.

29. DeLorenzo C, Kumar JS, Zanderigo F, et al. Modeling considerations for in vivo quantification of the dopamine transporter using [(11)C]PE2I and positron emission tomography. *J Cereb Blood Flow Metab* 2009; 29: 1332–1345.

30. Hirvonen J, Johansson J, Teräs M, et al. Measurement of striatal and extrastriatal dopamine transporter binding with high-resolution PET and [11C]PE2I: quantitative modeling and test-retest reproducibility. *J Cereb Blood Flow Metab* 2008; 28: 1059–1069.

31. Slifstein M, Parsey RV and Laruelle M. Derivation of [(11)C]WAY-100635 binding parameters with reference tissue models: effect of violations of model assumptions. *Nucl Med Biol* 2000; 27: 487–492.